Time series analysis of remotely sensed snow cover data: Revealing permafrost thermal state and vegetation dynamics

Sebastian Roessler, Andreas Dietz & Samuel Schilling

German Aerospace Center, German Remote Sensing Data Center, Wessling, Germany

ABSTRACT

Snow cover plays a crucial role in climate change and is considered an essential climate variable by the Global Climate Observing System (GCOS). To accurately monitor daily snow cover extent, optical medium-resolution remote sensing systems like MODIS and VIIRS are employed. DLR's Global SnowPack (GSP) product, derived from daily MODIS/VIIRS snow cover data, addresses data gaps caused by clouds or polar night, providing gap-free daily datasets since February 2000. The extended time series allows the identification of trends in snow cover duration (SCD), which has implications for the thermal state of permafrost soils and vegetation dynamics. Snow acts as an insulating barrier against colder winter air temperatures, enabling the underlying permafrost layer to retain higher temperatures. The 23-year dataset of SCD data from GSP allows both the determination of a long-term average and the derivation of trends. We compared both the mean SCD and the trend with annual changes in parameters describing horizontal and vertical permafrost extent, as well as changes in land cover classifications (both provided by ESA CCI). Regarding "Greening of the Arctic" we found changes in land cover classes, but in the observed period since 2000 there was little dynamism, and this is only slightly reflected in the SCD. Obvious developments were found in the thermal state of the permafrost – mainly degradation, but increases were also noted, similar to the positive trends in snow cover duration. Changes in Active Layer Thickness (ALT) could be best explained with SCD changes. Overall, additional data are needed to make quantitative predictions about permafrost development using SCD.

1 INTRODUCTION

The Arctic region is undergoing rapid and profound transformations driven by the escalating impacts of climate change (Lemke et al. 2007). In this context, permafrost degradation has emerged as a vital indicator of ecological shifts. These shifts involve the deepening of the active layer (Streletskiy et al. 2015), the greening of the Arctic (Myers-Smith et al. 2020, Shijin and Xiaoqing 2023), changes in precipitation (Wang et al. 2021), and increasing air temperatures (Guo and Wang 2016). These intertwined changes, along with their complex dynamics, demand innovative monitoring approaches that can unravel their connections and implications. An invaluable tool in this pursuit is the analysis of time series data on snow cover duration, as derived from Moderate Resolution Imaging Spectroradiometer (MODIS) imagery. This study explores the potential of MODIS-derived variability and trends in snow cover duration to monitor changes in the permafrost thermal regime and the associated land cover changes, shedding light on their interconnectedness and broader implications.

Permafrost, the frozen ground underlying vast Northern Hemisphere regions, is a sensitive indicator of climate change. Its degradation leads to the release of greenhouse gases, accelerating global warming and triggering cascading environmental consequences. Monitoring permafrost's spatial extent and thermal conditions, including active layer thickness, is pivotal for gauging the pace and magnitude of these changes (Xu and Zhuang 2023).

Parallel to permafrost degradation, the Arctic landscape is experiencing a visible transformation in land cover and vegetation patterns, collectively referred to as "Arctic greening". This phenomenon involves increased vegetation growth, shifts in vegetation composition, and altered ecosystem distributions (Bhatt et al. 2013). These changes have the potential to amplify permafrost degradation, as shifts in land cover can alter energy exchange processes and temperature regimes, further exacerbating thawing dynamics (Langer et al. 2013).

Effectively monitoring the complex interplay between permafrost dynamics and land cover changes in the expansive and remote Arctic region presents great challenges. Ground-based measurements are limited in their spatial coverage and are often unable to capture the full extent of changes. This underscores the importance of remote sensing technologies in addressing these challenges. Remote sensing provides comprehensive, consistent, and spatially extensive data, enabling researchers to monitor changes across vast landscapes (Jorgenson and Grosse 2016).

Among the myriad of remote sensing parameters, snow cover duration emerges as a valuable indicator of climate change effects on permafrost and land cover. Snow cover duration directly influences the ground's thermal regime, impacting permafrost thawing rates (Domine et al. 2022). Concurrently, it influences the timing and duration of vegetation growth, thus linking snow cover dynamics with land cover changes.

MODIS, with its daily global coverage, presents an ideal data source for analyzing snow cover dynamics (Dietz et al. 2012). By examining variability and trends in snow cover duration derived from MODIS imagery, researchers can gain insights into the Arctic environment's transformations (Muster et al. 2015). The consistent, long-term records provided by MODIS facilitate the identification of temporal patterns and potential relationships between snow cover duration and broader environmental changes.

https://doi.org/10.52381/ICOP2024.158.1

This study seeks to address two fundamental research questions:

1. Can MODIS-derived variability and trends in snow cover duration serve as indicators of changes in the permafrost thermal regime? By analyzing the relationships between snow cover duration and active layer thickness, we can investigate whether longer snow-free periods contribute to increased permafrost degradation. This question aims at the connection between the dynamics of the snow cover and the stability of the permafrost.
2. Can MODIS-derived snow cover duration data be used to monitor land cover changes associated with Arctic greening? Investigating correlations between snowmelt timing, snow-free periods, and vegetation growth patterns can provide insights into how shifts in snow cover influence the timing and extent of Arctic greening. This research question addresses the relationship between snowpack dynamics and changes in vegetation composition and spatial distribution.

Due to the availability of already existing high-quality datasets, this contribution uses data from the ESA Climate Change Initiative (CCI), like permafrost data mainly derived from MODIS LST and land cover classification, that contains MODIS NDVI data among others instead of the raw data products.

2 Dataset and Methods

2.1 Snow Cover

The DLR product GSP (Dietz et al. 2015) forms the database for the global daily snow cover. It is based on the daily MODIS snow products (Hall et al. 2002) from the Terra and Aqua platforms and essentially represents a method of gap filling (through clouds or the polar night). In four consecutive steps, gaps are first filled by combining the daily snow product of both platforms. In the second step, the remaining gaps are first filled with data from the previous day and then with those from the following day. A digital elevation model is then used to determine the upper snow line (elevation above which only snow occurs) and the lower snow line (elevation below which only snow-free pixels occur). All pixels above or below are determined accordingly. The last step is a gradual filling with the data from the previous days. This results in a gap-free global snow coverage daily.

From this daily binary information on snow cover extent, the time within which a pixel was snow-covered is determined: the snow cover duration (SCD). The SCD can be further used to determine long-term trends, but strong deviations in near real-time can also be used to detect natural hazards. Linking SCD to river runoff can be used to identify extreme hydrological events (floods or droughts) at an early stage. This was successfully shown for rivers in Lapland. (Rößler et al. 2021). Figure 1 shows the arithmetic mean of the annual snow cover duration for the northern hemisphere.

The annual deviation from this long-term average is further examined in the trend analysis.

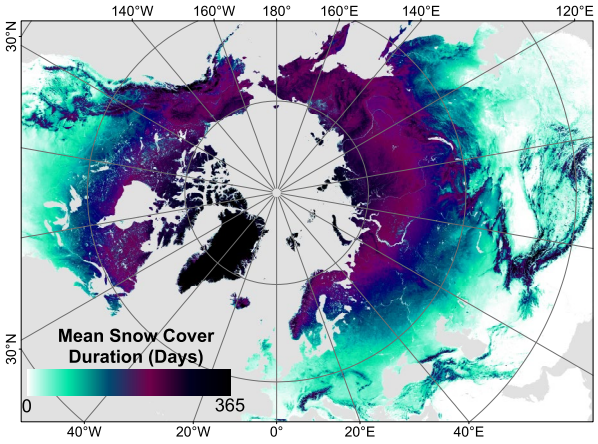

Figure 1. Mean annual snow cover duration in the northern hemisphere.

2.2 Permafrost

The permafrost data used within this study are derived from the ESA Climate Change Initiative Project "Permafrost_CCI" (Obu et al. 2021). We used the Permafrost Year 3 Climate Research Data Package available at the CEDA archive (https://archive.ceda.ac.uk/, accessed on 06/21/2023). For the years 2000–2019 (since the start of MODIS Terra) we obtained the datasets for Permafrost Fraction (PFR) and Active Layer Thickness (ALT).

The datasets have a spatial resolution of 1 km and are available as the arithmetic mean of the horizontal (PFR) and vertical (ALT) permafrost extent for each year. For the PFR dataset, the continuous coverage values (from 0 to 100%) were divided into seven evenly distributed classes. This gives the values 0 for permafrost-free areas and 14, 29, 43, 57, 71, 86, and 100, which each represent the area percentage of the permafrost cover. Since we have no continuous values, Figure 2 shows the modal value of the PFR time series from 2000 to 2019.

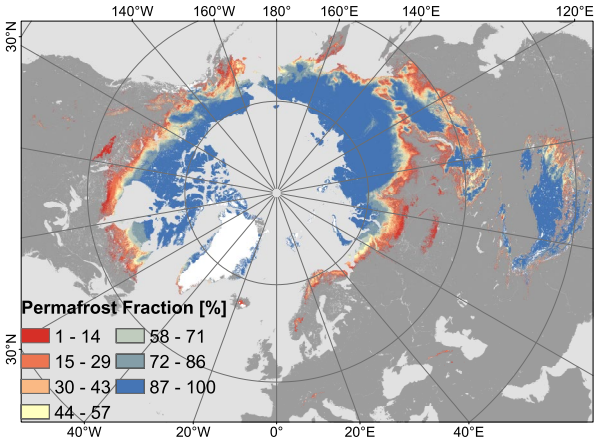

Figure 2. Permafrost Fraction (PFR) modal value for the period 2000–2019.

The ALT dataset reflects the continuous depth of the thaw layer in meters. However, since 99% of the depths do not exceed 2.55 m, we converted them to cm and also divided this range into seven classes with the same number of pixels (quantile subdivision) of the overall mean ALT value for examination. The resulting ranges are 1–40, 41–56, 57–73, 74–89, 90–108, 109–141 and 142–255 cm. Figure 3 shows the classes of mean annual ALT.

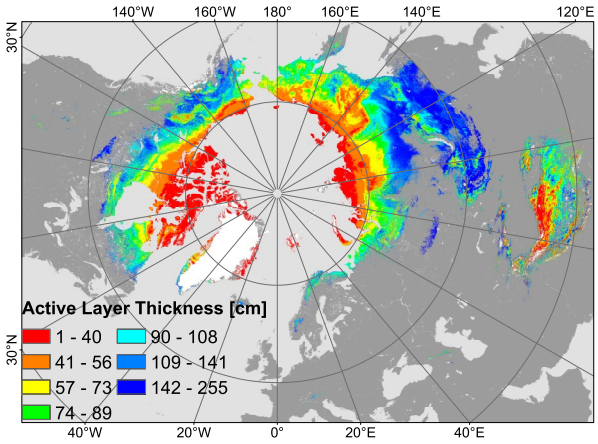

Figure 3. Map showing the quantile-based classification of the mean annual active layer thickness.

These two permafrost classifications (horizontal and vertical) form the basis for the following investigations of the 20-year time series.

2.3 Land Cover

Land cover (LC) time series data are also obtained from the ESA Climate Change Initiative (CCI). The dataset (Bontemps et al. 2013) distinguishes 37 land cover classes, although we have reduced these to 22 by merging the subclasses. Based on the overall extent of the seven PFR classes, we found that only six land cover classes make up the majority of land coverage (about 75%). Figure 4 shows their composition depending on the PFR.

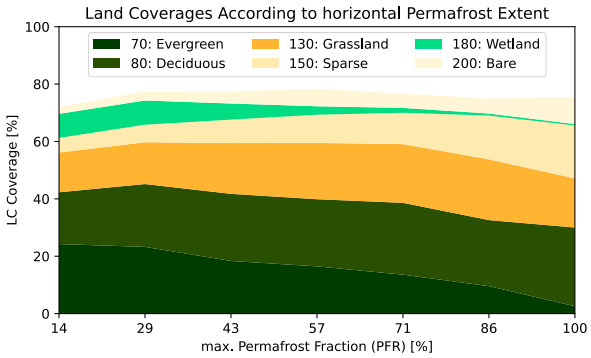

Figure 4, Change of the six permafrost land cover classes composition for the seven PFR classes (horizontal permafrost extent).

Figure 5 shows the modal distribution of these classes for the years 2000 to 2019.

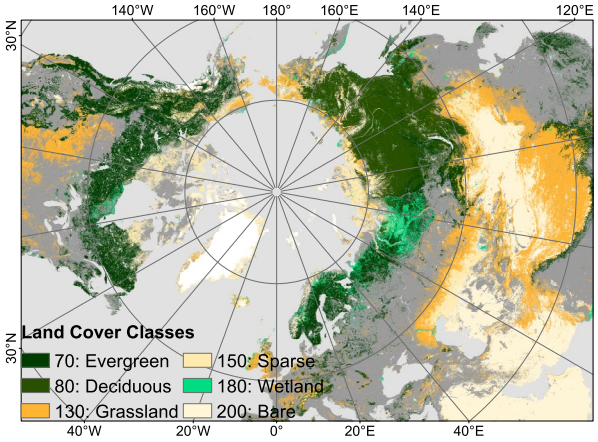

Figure 5, Modal distribution of the six selected permafrost land cover classes.

2.4 Time Series Analysis

2.4.1 Snow Cover

A Mann–Kendall test was performed to analyze the statistical significance of the trends of SCD (Hussain and Mahmud 2019). In this analysis, the null hypothesis (H0), stating the absence of a monotonic trend was tested against three alternatives: (i) a positive monotonic trend, (ii) a negative monotonic trend, or (iii) no monotonic trend. The null hypothesis is rejected if the *p*-value is below the chosen significance level of 0.1. Autocorrelation was absent in the datasets, allowing the use of the null hypothesis test. The magnitude of the trend was determined by the Theil-Sen slope, which, in contrast to linear regression, is more robust against outliers.

2.4.2 Permafrost and Land Cover

Since both the data on permafrost extent and that on land cover are either discrete or categorical, the continuous data on Active Layer Depths were also classified to enable a uniform procedure.

We are interested in the changes that occur from one year to another. It is then determined for each class how many pixels have changed to another class at this time. This gives us an array with the dimensions $[x, y, z]$, where x and y has the same dimensions and describe the number of classes. The third axis $z$describesthe time axis (i.e., 19 annual transitions). For each element of this array, mean snow cover information is then extracted (SCD and slope).

For each variable examined, we get $x * y * z$ results, which can either be displayed as an average over the zz-axisor can span a 2-dimensional point space with the axes SCD and slope to delineate transition regions. These transition zones are an ellipse surrounding an area showing the mean SCD and Theil-Sen slope (± standard deviation) for each group. The latter will be shown in this paper to identify possible separation possibilities.

3 RESULTS AND DISCUSSION

3.1 Snow Cover Dependencies

3.1.1 Development of Snow Cover

The SCD trend is calculated from the snow cover duration of each hydrological year (beginning of meteorological autumn to the end of meteorological summer) from 2000 to 2019 and the slope is given in days per year. The major part of the northern hemisphere shows a decrease in snow cover duration for the full year. The pixel-based slopes are shown in Figure 6.

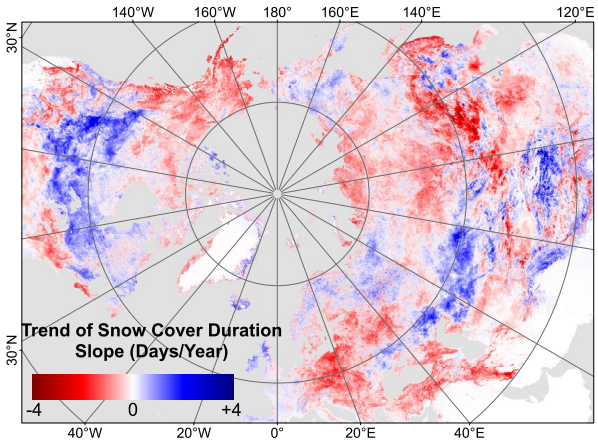

Figure 6. Theil-Sen slope of the SCD development.

However, especially in continental regions in North America and Asia, there has been an increase in the snow cover duration over large areas. For example, the Central Asian Syr Darya Lake Balkash and the Nelson River in North America had a significant increase in November.

3.1.2 Snow Cover of Classes

The next step was to analyze the snow cover variability of the permafrost and land cover classes. We start again with the horizontal permafrost extent (Figure 7).

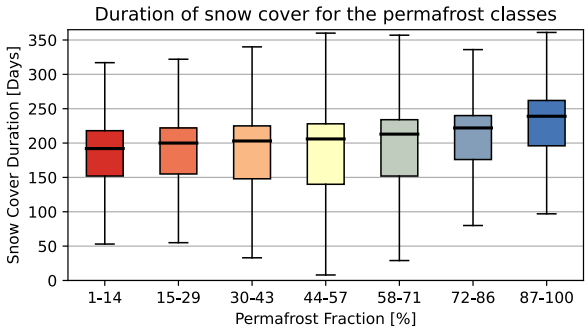

Figure 7. Snow cover duration boxplots for the Permafrost Area Fraction classes.

We see a clear decrease in the SCD with a decreasing area percentage of permafrost. The same can be observed for the vertical permafrost extent (ALT; Figure 8).

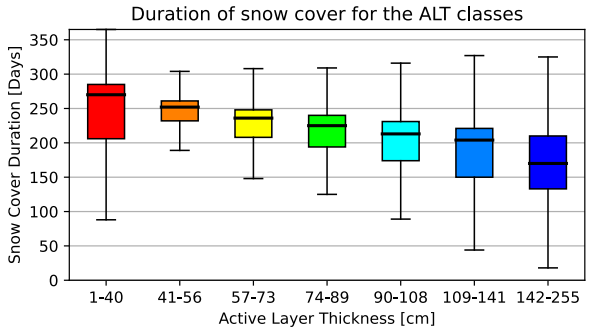

Figure 8. Snow cover duration boxplots for the Active Layer Thickness classes.

It is noteworthy here that the boxes (interquartile range) of classes 41–56, 57–73, and 74–89 are small and statistically different and should allow a good distinction between each other. A much clearer variability can be seen in the land cover classes (Figure 9).

In particular, “Grassland” (130) and “Bare” (200) show high SCD variability.

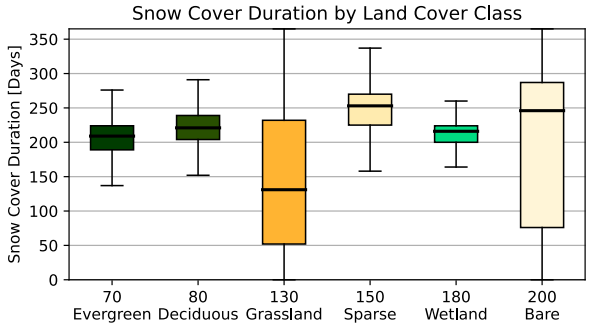

Figure 9. Snow cover duration boxplots for the land cover classes.

3.2 Findings from the Time Series

All work aims at detecting permafrost degradation using snow cover duration data. To give us an initial overview, a different map was created in which the extent of the permafrost in the year 2000 is compared with the situation 20 years later. To do this, we looked at the difference between the PFR and the ALT of both years. In this simplified approach, the pixel was then recognized as degraded permafrost if the ALT difference was above 50 cm, or if the PFR difference was more than 24%. The alarming result can be seen in Figure 10.

In the following, we will take a closer look at the changes. The changes are presented in two ways: the matrix figures show to which class classes will change (or what percentage of pixels remain the same). From this, you can already tell whether degradation is taking place. In the ellipse figures, only the changing pixels are considered and their snow cover duration and trend are shown to determine whether these parameters can already indicate future developments.

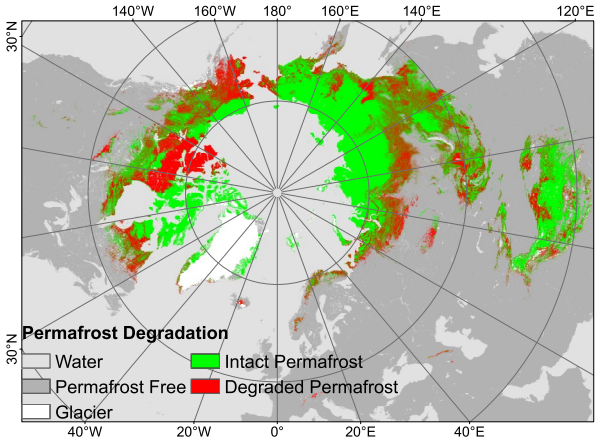

Figure 10. Maps showing permafrost degradation between 2000 and 2019 (either PFR or ALT).

3.2.1 *Permafrost Area Fraction*

Figure 11 shows the mean transitions of the 7 PFR classes (only maximum percentage is shown) over the 20 years. The matrix reads as follows: On the x-axis, you will find the class affiliation in the current year, and on the y-axis the class affiliation in the previous year. If you take the PFR value of 57 as an example, in the next year 94.03% will still belong to this class, 2.21% of the pixels have moved up to the next higher class (71) and 3.42% to the next lower class (43).

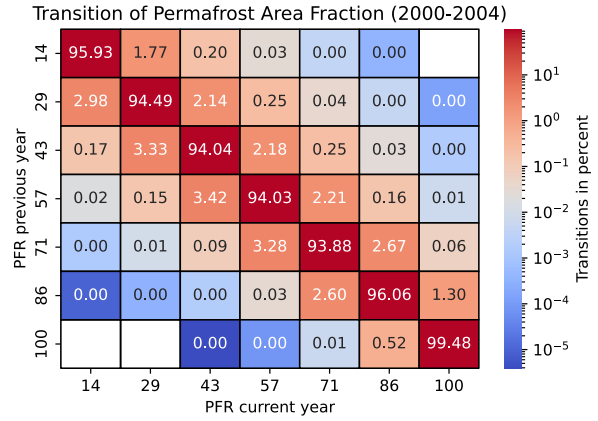

Figure 11. Transition diagram of the Permafrost Area Fraction (PFR).

In general, we see that there is a tendency towards a decrease in the permafrost fraction. Also, the transitions occur mostly in the neighboring classes. To find out how the class transition is connected to SCD and its development, the changing pixels are displayed as a 2-dimensional point cloud (where SCD is shown on the x-axis and the slope on the y-axis). The ellipses show the standard deviation around the respective mean values. The more clearly the ellipses can be distinguished, the better the separation. From Figure 12 you can see that the areas of the PFR transition largely overlap and are therefore not recognizable only by SCD and its development.

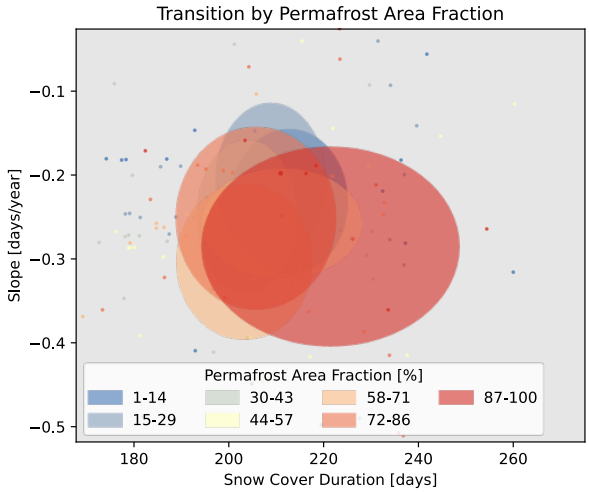

Figure 12. Snow coverage metrics for the transition regions of the PFR classes

In addition to the large overlap area of almost all classes with snow cover duration between 190 and 220 days and a slope of -0.2 to 0.3 days/year, the class "PFR = 100%" in the range of SCD > 230 and a slope > -0.2 stands out.

3.2.2 *Active Layer Thickness*

As with the horizontal permafrost classes, we also find a predominant increase in the Active Layer Thickness. This is visible in the transition diagram of ALT (Figure 13).

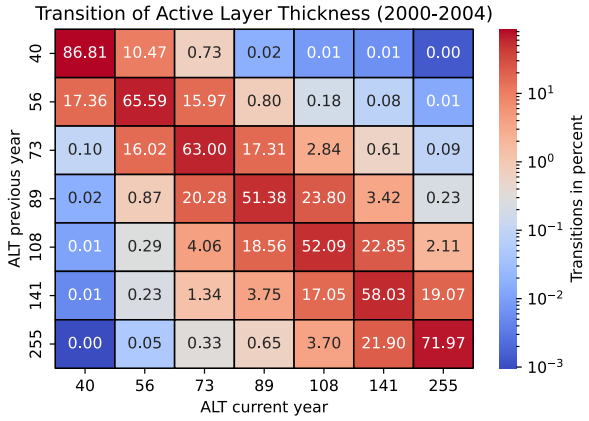

Figure 13. Transition diagram of the development of the Active Layer Thickness (ALT).

What we also see is a stronger variability in ALT. In contrast to PFR, a maximum of 80% remain in the previous class, mostly around 50%.

To see whether this development is also reflected in the snow information, Figure 14 shows the transition regions for the final class affiliation.

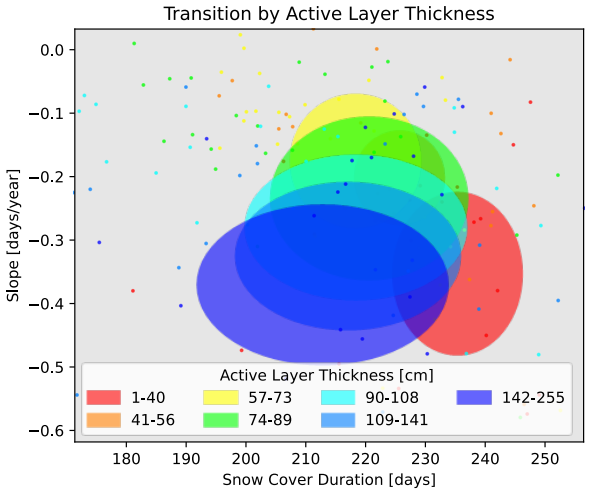

Figure 14. Snow coverage metrics for the transition regions of the ALT classes.

The smooth transitions are also reflected in the snow cover statistics. Although there is a large area of overlap between 210 and 230 days SCD and a slope between -0.2 and -0.4 days/year, there is a clear tendency for the ALT to increase more with lower initial snow cover duration and a larger slope. Only the lowest ALT (1–40 cm) occupies a distinct region between 230 and 240 days SCD and slopes ranging from 0.2 to 0.45 days/year. Studies in Alaska confirm these short-term changes, a shortening of the SCD by 10 days led to a temperature increase of several degrees, but they also speak of the fact that the effect on ALT is low (Ling and Zhang 2003).

3.2.3 Land Cover

In connection with the topic "Greening of the Arctic," we are interested in whether the information on snow cover can provide information about changing land cover. However, it is apparent from Figure 15 that these changes take longer than the observed 20 period.

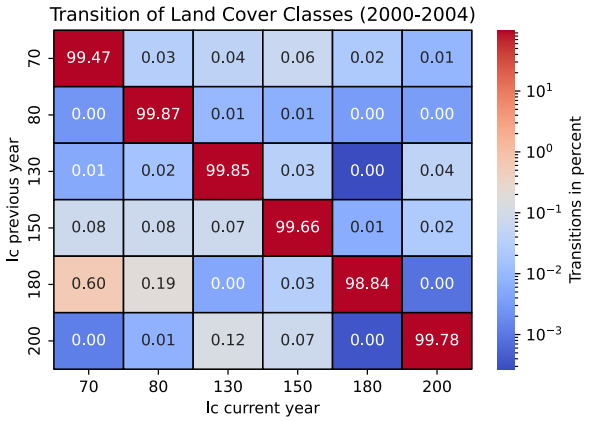

Figure 15. Transition diagram of the Land Cover (LC).

Class membership is very stable and few transitions have taken place. If we now look at the snow cover metrics in which these transitions occur (Figure 16), it becomes clear that “Bare” (200) or ”Sparse” (150) in particular overlap.

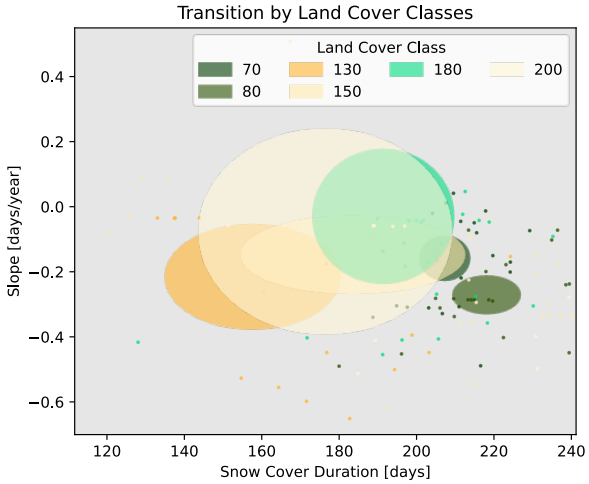

Figure 16. Snow coverage metrics for the transition regions of the Land Cover classes.

“Deciduous” (80) is best distinguished from the others because it has a relatively long average SCD of 210 to 230 days and the slope is also in a narrow range of between -0.2 and -0.3 days/year. Shorter snow cover durations (135–180 days) and a larger area slope (-0.5 to -3.5 days/year) are occupied by “Grassland” (130), which is a typical element at average PFR (~50%).

4 DISCUSSION

Regarding the limitations, the following can be summarized. The spatial resolution of MODIS can be insufficient, especially in mountainous regions, the limitations by clouds are mitigated by using an advanced gap-filling method (i.e., GSP), but this is still an assumption. Although snow depth has a large influence on thermal insulation (Domine et al. 2022), optical remote sensing can only detect two-dimensional snow coverage. However, the filled GSP daily snow coverage can help downscale this information from passive microwave (Tanniru and Ramsankaran 2023) in the future. Another issue is the period in which the data are collected. The information provided by ESA CCI Permafrost is averaged over calendar years, but snow cover duration is based on hydrological years (meteorological autumn to summer). Recent studies show that changes in snow cover usually occur at the end of autumn/beginning of winter (Roessler and Dietz 2022). This annual update of land cover classes, for example, was also the reason why the ESA product was used and not specific circumarctic products such as the CAVM (Walker et al. 2005; Raynolds 2022).

In the results, we observed various relationships between snow cover duration and permafrost parameters. On the one hand, there is a strong connection between horizontal (PFR) and vertical (ALT) permafrost extent, and this is reflected in the average snow cover duration of the classes.

There are also some clear connections between the land cover classes: with increasing PFR, the class “Evergreen” (70) almost completely disappear and “Deciduous” (80) increases. The classes “Grassland” (130), “Sparse” (150), and “Bare” (200) also increase with increasing PFR. The high SCD variability of "Grassland" (130) and "Bare" (200) in Figure 9 can be explained by their broader use: "Grassland" includes arctic tundra and steppe, "Bare" includes the polar cold desert (high SCD) and the deserts (low SCD) of lower latitudes.

The transition tables were able to clearly show the time frame within which permafrost changes occur. As expected, the slowest changes occurred in land cover. What's interesting here is the transition from "Bare" (200) to "Sparse" (150) or even "Grassland" (130) — a sign of Arctic Greening, just like the expansion of the boreal coniferous forest (Myers-Smith et al. 2020). It is also interesting that changes occur in both directions (degradation predominates), which affects both PFR and ALT. This is consistent with the observed trend of SCD. ALT also turned out to be the most variable permafrost parameter. On the one hand, this is where most of the changes took place between the years, and on the other hand, this is where we could see the clearest connection with the SCD (in terms of both the mean SCD and the trend). This can be explained by the insulating effect of the snow cover, as we can assume that a longer-lasting snow cover is associated with greater snow thickness (better insulation).

Our first research question was whether it is possible to understand permafrost developments with the average snow cover duration and their trend. This does not seem possible for PFR (yet) but is possible for vertical permafrost extent (ALT). Our future approach will involve integrating meteorological data and potentially AI techniques to enhance the comprehensiveness of outcomes. Similarly, in the context of the second research question, the gradual adaptation of land cover to evolving climatic conditions introduces a temporal lag, challenging the real-time linkage between snow cover and processes like Arctic greening. But here too we were able to identify classes that show distinctive mean SCD and trend.

5 Conclusions

In this study, we utilized time series data from ESA CCI to analyze permafrost and land cover dynamics. Our objective was to detect permafrost degradation (due to decreasing permafrost area extent, active layer deepening, and arctic greening) and correlate them with MODIS snow cover data. Results consistently revealed permafrost degradation across active layer thickness, permafrost extent, and land cover classes.

Despite considerable variability in snow cover duration, we successfully identified regions with pronounced distinctions in both snow cover duration and SCD slope values during class transitions. This outperformed the resolution capabilities of lower-resolution sensors like passive microwave sensors.

Remote sensing-derived snow coverage data are a valuable tool to affirm permafrost degradation trends and augment spatial resolution relative to coarser sensors.

Nonetheless, this tool alone falls short of independently substantiating assertions regarding permafrost degradation and Arctic greening complexities. Subsequent steps involving meteorological data integration and AI-driven methodologies are imperative for a comprehensive understanding of these intricate dynamics.

6 References

Bhatt, U., Walker, D., Raynolds, M., Bieniek, P., Epstein, H., Comiso, J., Pinzon, J., Tucker, C., and Polyakov, I. 2013. ‘Recent Declines in Warming and Vegetation Greening Trends over Pan-Arctic Tundra’, *Remote Sensing* 5(9), pp. 4229–4254. doi:10.3390/rs5094229.

Bontemps, S., Defourny, P., Radoux, J., Van Bogaert, E., Lamarche, C., Achard, F., Mayaux, P., Boettcher, M., Brockmann, C., Kirches, G., et al. 2013. ‘Consistent global land cover maps for climate modelling communities: current achievements of the ESA’s land cover CCI’, in *Proceedings of the ESA living planet symposium*. Edinburgh, United Kingdom: ESA SP-722, pp. 9–13.

Dietz, A.J., Kuenzer, C., and Dech, S. 2015. ‘Global SnowPack: a new set of snow cover parameters for studying status and dynamics of the planetary snow cover extent’, *Remote Sensing Letters* 6(11), pp. 844–853. doi:10.1080/2150704X.2015.1084551.

Dietz, A.J., Wohner, C., and Kuenzer, C. 2012. ‘European Snow Cover Characteristics between 2000 and 2011 Derived from Improved MODIS Daily Snow Cover Products’, *Remote Sensing* 4(8), pp. 2432–2454. doi:10.3390/rs4082432.

Domine, F., Fourteau, K., Picard, G., Lackner, G., Sarrazin, D., and Poirier, M. 2022. ‘Permafrost cooled in winter by thermal bridging through snow-covered shrub branches’, *Nature Geoscience* 15(7), pp. 554–560. doi:10.1038/s41561-022-00979-2.

Guo, D. and Wang, H. 2016. ‘CMIP5 permafrost degradation projection: A comparison among different regions’, *Journal of Geophysical Research: Atmospheres* 121(9), pp. 4499–4517. doi:10.1002/2015JD024108.

Hall, D.K., Riggs, G.A., Salomonson, V.V., DiGirolamo, N.E., and Bayr, K.J. 2002. ‘MODIS snow-cover products’, *Remote Sensing of Environment* 83(1–2), pp. 181–194. doi:10.1016/S0034-4257(02)00095-0.

Hussain, M. and Mahmud, I. 2019. ‘pyMannKendall: a python package for non parametric Mann Kendall family of trend tests’, *Journal of Open Source Software* 4(39), 1556. doi:10.21105/joss.01556.

Jorgenson, M.T. and Grosse, G. 2016. ‘Remote Sensing of Landscape Change in Permafrost Regions’, *Permafrost and Periglacial Processes* 27(4), pp. 324–338. doi:10.1002/ppp.1914.

Langer, M., Westermann, S., Heikenfeld, M., Dorn, W., and Boike, J. 2013. 'Satellite-based modeling of permafrost temperatures in a tundra lowland landscape', *Remote Sensing of Environment* 135, pp 12–24. doi:10.1016/j.rse.2013.03.011.

Lemke, P., Ren, J., Alley, R.B., Allison, I., Carrasco, J., Flato, G., Fujii, Y., Kaser, G., Mote, P., Thomas, R.H., and Zhang, T. 2007. 'Observations: Changes in Snow, Ice and Frozen Ground', in S. Solomon et al. (eds.), *Climate Change 2007: The Physical Science Basis. Contribution of Working Group 1 to the Fourth Assessment Report of the Intergovernmental Panel on Climate Change*. Cambridge, United Kingdom: Cambridge University Press.

Ling, F. and Zhang, T. 2003. 'Impact of the timing and duration of seasonal snow cover on the active layer and permafrost in the Alaskan Arctic', *Permafrost and Periglacial Processes*, 14(2), pp. 141–150. doi:10.1002/ppp.445.

Muster, S., Langer, M., Abnizova, A., Young, K.L., and Boike, J. 2015. 'Spatio-temporal sensitivity of MODIS land surface temperature anomalies indicates high potential for large-scale land cover change detection in Arctic permafrost landscapes', *Remote Sensing of Environment* 168, pp. 1–12. doi:10.1016/j.rse.2015.06.017.

Myers-Smith, I.H., Kerby, J.T., Phoenix, G.K., Bjerke, J.W., Epstein, H.E., Assmann, J.J., et al. 2020. 'Complexity revealed in the greening of the Arctic', *Nature Climate Change* 10(2), pp. 106–117. doi:10.1038/s41558-019-0688-1.

Obu, J., Westermann, S., Barboux, C., Bartsch, A., Delaloye, R., Grosse, G., et al. 2021. 'ESA Permafrost Climate Change Initiative (Permafrost_cci): Permafrost Ground Temperature for the Northern Hemisphere, v3.0', *NERC EDS Centre for Environmental Data Analysis*. Available at: https://data-search.nerc.ac.uk/geonetwork/srv/eng/catalog.search#/metadata/6e2091cb0c8b4106921b63cd5357c97c.

Raynolds, M. 2022. *Raster Circumpolar Arctic Vegetation Map*, Mendeley Data, version 1. doi:10.17632/c4xj5rv6kv.1.

Roessler, S. and Dietz, A.J. 2022. 'Development of Global Snow Cover—Trends from 23 Years of Global SnowPack', *Earth* 4(1), pp. 1–22. doi:10.3390/earth4010001.

Rößler, S., Witt, M.S., Ikonen, J., Brown, I.A., and Dietz, A.J. 2021. 'Remote Sensing of Snow Cover Variability and Its Influence on the Runoff of Sápmi's Rivers', *Geosciences* 11(3), 130. doi:10.3390/geosciences11030130.

Shijin, W. and Xiaoqing, P. 2023. 'Permafrost degradation services for Arctic greening', *CATENA*, 229, 107209. doi:10.1016/j.catena.2023.107209.

Streletskiy, D., Anisimov, O., and Vasiliev, A. 2015. 'Permafrost Degradation', in *Snow and Ice-Related Hazards, Risks, and Disasters*. Elsevier, pp. 303–344.

Tanniru, S. and Ramsankaran, R. 2023. 'Passive Microwave Remote Sensing of Snow Depth: Techniques, Challenges and Future Directions', *Remote Sensing* 15(4), 1052. doi:10.3390/rs15041052.

Walker, D.A., Raynolds, M.K., Daniëls, F.J.A., Einarsson, E., Elvebakk, A., Gould, W.A., Katenin, A.E., Kholod, S.S., Markon, C.J., Melnikov, E.S., Moskalenko, N.G., Talbot, S.S., Yurtsev, B.A.(†), et al. 2005. 'The Circumpolar Arctic vegetation map', *Journal of Vegetation Science* 16(3), pp. 267–282. doi:10.1111/j.1654-1103.2005.tb02365.x.

Wang, P., Huang, Q., Tang, Q., Chen, X., Yu, J., Pozdniakov, S.P., and Wang, T. 2021. 'Increasing annual and extreme precipitation in permafrost-dominated Siberia during 1959–2018', *Journal of Hydrology* 603, 126865. doi:10.1016/j.jhydrol.2021.126865.

Xu, Y. and Zhuang, Q. 2023. 'The importance of interactions between snow, permafrost and vegetation dynamics in affecting terrestrial carbon balance in circumpolar regions', *Environmental Research Letters* 18(4), 044007. doi:10.1088/1748-9326/acc1f7.